

Tropical Cyclone Eye Thermodynamics

H. E. WILLOUGHBY

Hurricane Research Division, AOML/NOAA, Miami, Florida

(Manuscript received 10 June 1997, in final form 17 February 1998)

ABSTRACT

In intense tropical cyclones, sea level pressures at the center are 50–100 hPa lower than outside the vortex, but only 10–30 hPa of the total pressure fall occurs inside the eye between the eyewall and the center. Warming by dry subsidence accounts for this fraction of the total hydrostatic pressure fall. Convection in the eyewall causes the warming by doing work on the eye to force the thermally indirect subsidence.

Soundings inside hurricane eyes show warm and dry air aloft, separated by an inversion from cloudy air below. Dewpoint depressions at the inversion level, typically 850–500 hPa, are 10–30 K rather than the ~100 K that would occur if the air descended from tropopause level without dilution by the surrounding cloud. The observed temperature and dewpoint distribution above the inversion can, however, be derived by ~100 hPa of undilute dry subsidence from an initial sounding that is somewhat more stable than a moist adiabat. It is hypothesized that the air above the inversion has remained in the eye since it was enclosed when the eyewall formed and that it has subsided at most a few kilometers. The cause of the subsidence is the enclosed air's being drawn downward toward the inversion level as the air below it flows outward into the eyewall. Shrinkage of the eye's volume is more than adequate to supply the volume lost as dry air is incorporated into the eyewall or converted to moist air by turbulent mixing across the eye boundary.

The moist air below the inversion is in thermodynamic contact with the sea surface. Its moisture derives from evaporation of seawater inside the eye, frictional inflow of moist air under the eyewall, and from moist downdrafts induced as condensate mixes into the eye. The moist air's residence time in the eye is much shorter than that of the dry air above the inversion. The height of the inversion is determined by the balance between evaporation, inflow, and inward mixing on one hand and loss to the eyewall updrafts on the other.

1. Introduction

The lowest surface pressure in a hurricane coincides with the axis of vortex rotation inside the eye. The swirling wind—the tangential component of the wind vector in storm-centered cylindrical coordinates—increases with distance outward from the axial stagnation point to the radius of maximum wind at the inner edge of the eyewall. The eyewall, a ring of cumulonimbus convection, surrounds the eye and contains the sharpest radial pressure gradient nearly coincident with strongest wind. Because the eyewall slopes outward, the eye is approximately an inverted, truncated cone. The air aloft in the eye is clear, warm, and dry, separated by an inversion from more moist, usually cloudy air near the surface (Jordan 1952). Subsidence is the source of the eye's warmth and dryness. Subsidence-induced adiabatic warming increases the thickness between the fixed tropopause height and the surface, lowering the hydrostatic surface pressure at the vortex center as the cyclone in-

tensifies. Because the subsiding air is warmer than any other air in the cyclone, the descent must consume energy released elsewhere in the storm.

Balanced models predict, and observations confirm, that the most rapid pressure falls are confined to the area inside the eyewall wind maximum (Shapiro and Willoughby 1982; Schubert and Hack 1982; Willoughby et al. 1982; Willoughby 1990). Tightening of the pressure gradient across the wind maximum causes the wind to increase at, and inward from, the radius of maximum wind so that the eyewall contracts as the wind strengthens. Dynamically or thermodynamically forced outflow from the lower part of the eye into the eyewall causes the sinking and adiabatic warming, and hence the pressure falls. Inside the eye, where the wind increases with radius, air must subside from above to replace the loss to the eyewall because horizontal motion is constrained by the strong radial gradient of angular momentum. On the other hand, outside the eyewall, where the wind decreases with radius and the radial angular momentum gradient is weaker, air can converge horizontally above the friction layer to replace the mass carried aloft by convection. This midlevel inflow from large radius supplies the angular momentum necessary to increase the swirling wind, in contrast with the frictional inflow near the surface, which extracts moist enthalpy from the sea

Corresponding author address: Dr. H. E. Willoughby, Hurricane Research Division AOML/NOAA, 4301 Rickenbacker Causeway, Miami, FL 33143.
E-mail: willoughby@aoml.noaa.gov

surface and feeds it into the convection, but can supply little excess angular momentum (Ooyama 1969, 1982).

The pressure fall between the eyewall and the center accounts for only part of the total difference between the undisturbed surface pressure outside the storm and minimum sea level pressure (MSLP) at the center. The process of bringing the late-summer tropical troposphere into thermodynamic equilibrium with the sea surface at 28°–30°C, taking into account the elevation of equivalent potential temperature as the pressure declines, can produce hydrostatic pressures as low as the minimum sea level pressures of the most intense tropical cyclones. Thermodynamic arguments (e.g., Miller 1958; Emanuel 1986) that relate maximum possible intensity of hurricanes to sea surface temperature (SST) are essentially elaborations of this result. Nevertheless, the moist adjustment process is only part of the story because the tropospheric column in real tropical cyclones is generally undersaturated except in organized convection, such as the eyewall, in the stratocumulus deck that caps the surface boundary layer, or in the outflow anvil near the tropopause. An airplane flying outside of convection in the midtroposphere typically encounters precipitation, but little cloud. The eye itself is often clear, apart from boundary layer stratocumulus. This observation applies most consistently to intense tropical cyclones that are continuing to intensify. Once intensification stops, but before the pressure has risen appreciably, the eye typically fills with cloud (Jordan 1961).

The conventional view of the eye's thermodynamics is that air detrains from the top of the eyewall and sinks inside the eye to the lower troposphere where it is entrained back into the eyewall. Inward mixing from the eyewall is hypothesized to force the subsidence and maintain the moisture and momentum budgets of the subsiding air (Miller 1958; Malkus 1958; Holland 1997). In this interpretation, the recirculation is rapid enough to replenish the eye's volume many times over the hurricane's lifetime. The original argument for rapid replenishment of the air in the eye was that the calm air inside the eye did not appear to share in the translation of the vortex as a whole (Malkus 1958), and that the eye moved by continuously reforming. More recent observations from aircraft equipped with inertia navigation equipment show clearly that the low-level wind is a superposition of circulation about the axis of rotation and the translation of the axis (Willoughby and Chelmon 1982) so that it is kinematically possible for a mass of air to move with the eye.

Here observed eye soundings are examined; they suggest that the dry air above the inversion has a long lifetime inside the eye, experiences only a few kilometers total subsidence, and mixes only weakly with the moist air from the eyewall. The air below the inversion seems, by contrast, to derive largely from the eyewall, or from frictional inflow layer below it, through a complicated process of mixing and evaporatively driv-

en subsidence. A conceptual model based upon this interpretation can synthesize observed eye soundings and calculate realistic hydrostatic pressure falls from the eyewall inward to the axis of vortex rotation.

2. Observed eye soundings

Eastern Pacific Hurricane Olivia formed from a disturbance on the ITCZ on 19 September 1994. It reached hurricane intensity early on 24 September, less than two days after it had become a tropical storm (Pasch and Mayfield 1996). Late on the 24th at 1922 UTC, the National Oceanic and Atmospheric Administration's WP-3D research aircraft began two days of operations in the hurricane, providing clear documentation of the influences of environmental wind shear and SST on intensity and structure. When the aircraft arrived in Olivia, the MSLP had fallen to 949 hPa as the storm moved in weak easterly environmental wind shear over warm water with SST >28°C. Olivia continued to intensify throughout the 4 h that the airplanes remained in the storm on the first day. Subsequently, the MSLP appeared to reach a minimum overnight at about 1200 UTC on the 25th. When the aircraft returned at 2021 UTC on the 25th, Olivia's MSLP was 924 hPa, lower than on the previous day, but the storm filled throughout the rest of the flight in response to cooler SST and somewhat stronger, then southwesterly, shear caused by an upper low northeast of the hurricane. By the time the aircraft left the storm on the second day, the MSLP had risen to 935 hPa.

A dropsonde observation in Olivia's eye at 2123 UTC on the 24th (Fig. 1a) is typical of intensifying tropical cyclones. It shows the expected inversion between 890 and 850 hPa, separating warm and dry air above from moist air below. In the moist air, the sounding follows a saturated adiabat down to 920 hPa and then a dry adiabat to the surface. Above the inversion, the dewpoint depression increases from 10 K at the top of the inversion to 12 K at 600 hPa, the top of the sounding. The temperature and dewpoint soundings both run generally parallel to moist adiabats in the dry air, but with 1–3 K perturbations. Equivalent potential temperature, θ_e , has a weak minimum value of 350 K near 700 hPa (Fig. 1b). It increases abruptly from 355 K at the top of the inversion layer to nearly 365 K at the bottom. The vapor mixing ratio decreases from 11 gm kg⁻¹ just above the inversion to about 7 gm kg⁻¹ at 600 hPa. The mixing ratio jumps to >20 gm kg⁻¹ downward across the inversion.

Saturation point analysis (Betts 1982) is a good tool for understanding eye thermodynamics. In undersaturated air, the saturation point is essentially the lifting condensation level determined by expansion of the parcel along a dry adiabat, keeping constant water vapor mixing ratio, until saturation is reached at pressure P_{SAT} and temperature T_{SAT} . In saturated air with suspended condensate, the saturation point is determined by com-

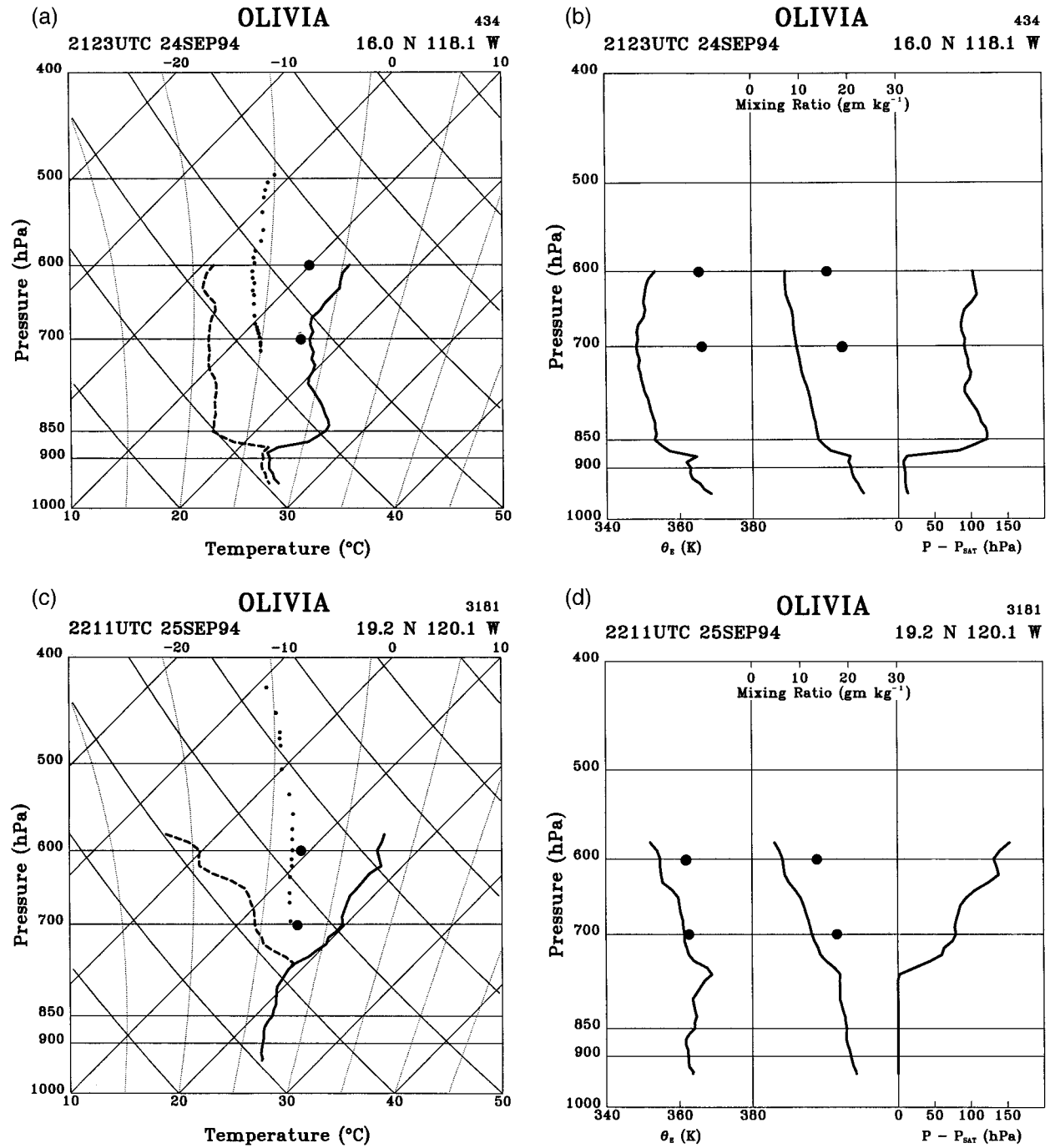


FIG. 1. (a) Skew T - $\log p$ diagram of the eye sounding in eastern Pacific Hurricane Olivia at 2123 UTC on 24 September 1994. Isotherms slope upward to the right; dry adiabats slope upward to the left; moist adiabats are nearly vertical curving to the left. Solid and dashed curves denote temperature and dewpoint, respectively. The smaller dots denote saturation points computed for the dry air above the inversion, and the two larger dots temperature observed at the innermost saturated point as the aircraft passed through the eyewall. (b) Equivalent potential temperature, θ_e , water vapor mixing ratio, and saturation pressure difference, $P - P_{SAT}$, as functions of pressure at 2123 UTC. (c) skew T - $\log p$ diagram of the eye sounding in Olivia at 2211 UTC on the 25th; and (d) θ_e , mixing ratio, and $P - P_{SAT}$ at 2211 UTC.

pression of the parcel along a moist adiabat until all of the suspended moisture has evaporated. The saturation point defines an air parcel's thermodynamics uniquely and is conserved under adiabatic processes. The saturation points of mixtures of parcels lie along a "mixing line" that joins the saturation points of the original parcels on a thermodynamic diagram.

Saturation points for parcels above the inversion in Olivia are indicated by dots in Fig. 1a. They lie within a degree or two of the moist adiabat that would pass through 25°C at 1000 hPa, corresponding to $\theta_e = 350$ K. The saturation pressure difference, $P - P_{SAT}$ in Fig. 1b [defined using the sign convention of Betts and Silva Dias (1979), the negative of that used by Betts (1982)], is 125 hPa above the inversion and decreases slowly with altitude. In the moist air below the inversion, $P - P_{SAT}$ is small, but not zero or negative, because the sonde apparently fell through a hole in the low-level stratocumulus.

Flight level measurements made as the aircraft passed through the eyewall provide estimates of the saturation points there. These estimates, indicated by larger dots in Fig. 1, are the temperature and pressure of the last saturated observations on entry to the eye or the first saturated observation on exit during the traverse of the eye when the sonde was deployed. They should lie close to a moist adiabat that passes through cloud base and should be close to T_{SAT} and P_{SAT} for eyewall air because most of the suspended condensate migrates outward across the outward sloping eyewall updraft to its outer edge where it falls out. The flight level eyewall θ_e is typically ~ 10 K warmer than θ_e in the eye, and the vapor mixing ratio is 10 gm kg^{-1} more. These measurements probably underestimate the differences between the eye and eyewall because of sensor wetting and dilution of the updraft near the boundary.

For undilute saturated parcels with some suspended condensate, the saturation points are determined by moving down the eyewall moist adiabat—which nearly parallels the actual eyewall sounding—until the suspended liquid has evaporated. About 20 hPa of compression are required to evaporate a gram of condensate per kilogram of dry air at the temperatures and pressures typical of the midtroposphere in hurricanes. Saturation points of mixtures between the cloudy eyewall air and dry air from the eye would lie along mixing lines that join the saturation points of the eye and eyewall. Thus, outward mixing of dry eye air would displace the saturation points in the cloudy eyewall updraft to the left, away from the moist adiabat characterizing the eyewall, toward the locus of saturation points inside the eye. Similarly, inward mixing of cloudy eyewall air would move the saturation points in the eye to the right, toward the eyewall sounding.

On the next day, the 25th, the soundings showed a clear signature of moisture mixing into the eye as the storm filled. Three soundings were taken that day at 2106, 2211, and 2349 UTC. Figures 1c and 1d show

the middle sounding. Although the air below the inversion is saturated, $P - P_{SAT}$ is plotted here (and subsequently) as though it were zero because no measurements of liquid water content are available. The dewpoint depression at the top of the sounding is 3 K greater than on the 24th. The temperature and dewpoint soundings form a "Y" shape that characterizes all three soundings on the 25th, in contrast with the earlier sharp inversion. The soundings show a clear progression: as the MSLP rose from 930 to 937 hPa in 2.7 h, the base of the inversion rose from 830 to 740 hPa with about half of the filling, but most of the inversion's ascent, occurring in the hour between the first two soundings. In all three soundings, the maximum $P - P_{SAT}$ was 150 hPa and occurred near 600 hPa. This value is 25 hPa greater than the maximum on the 24th and 250 hPa higher in the tropospheric column than the level (850 hPa) where the greatest $P - P_{SAT}$ occurred the day before. The value of $P - P_{SAT}$ at 600 hPa is also 40 hPa greater than the value of $P - P_{SAT}$ at the same altitude on the 24th. The greater $P - P_{SAT}$ near the top of the sounding reflects continuing descent in the eye as Olivia intensified overnight. The temporally constant maximum $P - P_{SAT}$ on the 25th suggests that low-level moistening of the eye was caused largely by inward mixing rather than by ascent due to convergence below the inversion. Comparison of the loci of saturation points between the two days is consistent with this interpretation. On the 24th the saturation points lay to the left of the $\theta_e = 350$ K moist adiabat; on the 25th they had migrated to the right of the same moist adiabat and approached the eyewall saturation points. The saturation points in the lower troposphere, where mixing was strongest, migrated farthest to the right. The cooling below 600 hPa can account for only about 1 hPa of the 7 hPa total pressure rise so that some other process—cooling above 600 hPa—must have been responsible for the higher hydrostatic central surface pressure.

Another possible mechanism for moistening the eye is evaporation of virga that falls into the eye, as described in Hurricane Edna (Kessler 1958). This process would move the saturation points down a moist adiabat, essentially parallel with the sounding that they define. Since the process would be nearly adiabatic, θ_e would not change. The heat of evaporation would come primarily from the air into which the virga fell, not from the hydrometeors. Thus, adiabatic evaporation would not leave a clear signature in the saturation points, and $P - P_{SAT}$ would underestimate the total descent. Nevertheless, low reflectivity inside the eye and sparse visual or photographic observations of virga at radii well inward from the eyewall argue generally against evaporation of virga as a major contributor to the eye's moisture budget. Snow or graupel falling into an eye covered with anvil cloud would be more difficult to observe

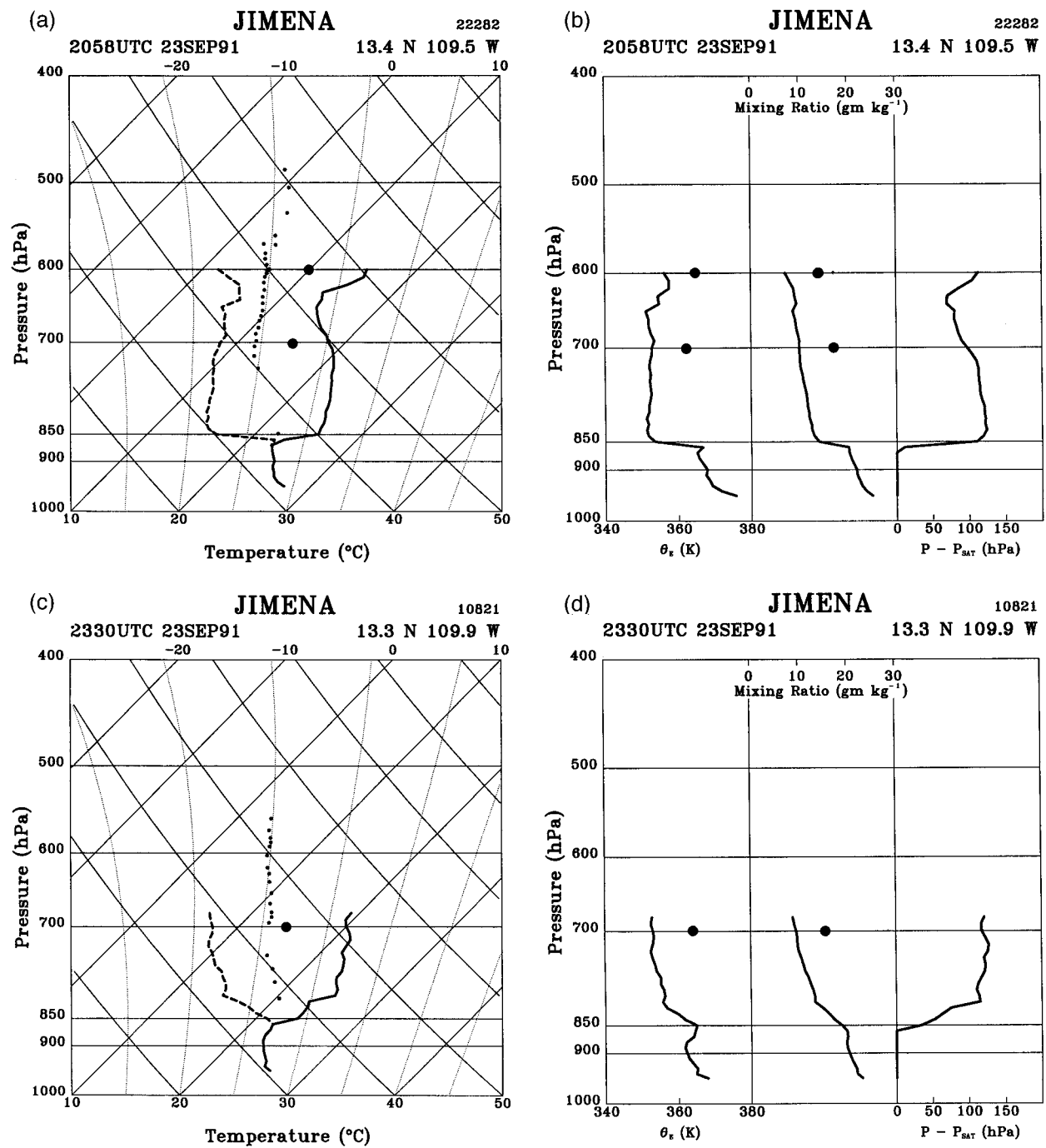


FIG. 2. As in Fig. 1 but for eastern Pacific Hurricane Jimena: (a) skew T -log p ; and (b) θ_e , mixing ratio, and $P - P_{SAT}$ at 2058 UTC on 23 September 1991. (c) skew T -log p ; and (d) θ_e , mixing ratio, and $P - P_{SAT}$ at 2330 UTC the same day.

visually or by radar so that this mechanism cannot be discounted completely.

Hurricane Jimena formed from an African wave that traversed Central America into the eastern Pacific, developed into a tropical depression on 20 September 1991, became a tropical storm on the 21st, and reached hurricane strength on the 22d (Rappaport and Mayfield

1992). The P-3s flew in Jimena on the 23d and 24th. Jimena's eye sounding at 2058 UTC on 23 September 1991, when Jimena's MSLP was 945 hPa (Fig. 2a), is almost the same as the first sounding in Olivia. It shows a sharp inversion near 850 hPa with warm, dry air aloft and moist air below. As before, the sounding in the moist air follows a moist adiabat downward from the inversion

and then a dry adiabat to the surface; the temperature and dewpoint soundings in the dry air run roughly parallel moist adiabats; and the dewpoint depressions in the dry air are about 10 K. The locus of the saturation points above the inversion lie more or less along the same $\theta_e = \sim 350$ K moist adiabat as in Olivia. Equivalent potential temperature, θ_e , has a minimum just above the inversion (Fig. 2b) with a slow increase with height above the inversion and then an abrupt increase from 350 K to nearly 370 K downward through the inversion. The minimum θ_e is >10 K cooler than θ_e in the eyewall, which is, in turn, about ~ 5 K cooler than the warmest value below the inversion. The saturation pressure difference is 130 hPa just above the inversion and decreases slowly with altitude.

Some of the depression of θ_e in the eye may result from radiative cooling of a degree or two per day, which can move the saturation points down a dry adiabat 100–200 m a day, or several hundred meters to a kilometer over the lifetime of a typical eye. This sounding also shows evidence of some mixing from the eyewall. The narrowing of the dewpoint depression at 620–650 hPa clearly stems from moistening and cooling as condensate mixes into the eye and evaporates. The saturation points for these levels are displaced to the right toward their counterparts in the eyewall, and θ_e increases to 355 K, still ~ 7 K cooler than the eyewall. Just above this level, the temperature increases and air dries, indicating subsidence, perhaps related to a 7 m s^{-1} downdraft that the aircraft data show in the south eyewall at 2258 UTC.

On the 23d and 24th, Jimena maintained nearly constant intensity in southwesterly shear over warm water. The only other sounding obtained in Jimena was 2.5 h after Fig. 2a at 2330 UTC (Fig. 2c). As the MSLP rose to 949 hPa, the base of the inversion remained at the same level, but the inversion layer became thicker. It extended from 860 hPa to 810 hPa so that the sounding became “Y” shaped somewhat like Olivia’s eye soundings on 25 September 1994. The saturation points in air formerly at the bottom of the dry layer moved to the right as the thickening inversion encroached on their level, and θ_e at 850 hPa increased from 350 to 365 K, the same value observed at 700 hPa in the eyewall. The saturation points above the inversion moved rightward as, despite the simultaneous cooling, inward mixing moistened the air enough to wipe out the θ_e minimum (Fig. 2d).

Since the structure and intensity of the storm remained fairly steady throughout both days, these soundings may represent different phases of an oscillating system rather than part of a long-term change. Eyewall convection in Jimena was cyclic with a period of one-half hour, close to the orbital period for air moving around the eye at the radius of maximum wind. The earlier sounding may represent a time when a recent pulse of convection had forced subsidence, whereas the later sounding may represent an interval between pulses

when mixing and inflow predominated. The time between the soundings is much longer than the observed period of the convection so that they are random samples of different phases of the oscillation, if this interpretation is correct.

Hurricane Hugo formed in the Atlantic from an African wave. It reached hurricane intensity on 13 September 1989 east of the Leeward Islands and intensified rapidly, becoming a category 5 hurricane on the 15th (Case and Mayfield 1990). The eye sounding in Hugo (Fig. 3a) at 1900 UTC on 15 September 1989, when Hugo’s MSLP was 922 hPa, is qualitatively much the same as Olivia’s and Jimena’s. In this case, the inversion is higher and thicker, extending from 790 hPa to 700 hPa. As in Jimena, the lowest θ_e , 350 K, and largest value of $P - P_{\text{SAT}}$, 175 hPa, lie at the top of the inversion (Fig. 3b); and the locus of the saturation points straddles the $\theta_e = 350$ K moist adiabat. Dewpoint depressions in the dry air inside the eye are nearly 20 K. The temperature and dewpoint profiles are only a little more stable than moist adiabats. Inward mixing from the eyewall between 550 and 630 hPa, appears to have caused a 5° decrease in dewpoint depression, saturation points’ displacement to the right of the $\theta_e = \sim 350$ K moist adiabat, and a 2–3 K increase in θ_e .

In the eyewall at 500 hPa, θ_e was 362 K based upon flight-level temperature of 2°C . At 890 hPa the eyewall, θ_e was much warmer, 375 K measured as the aircraft flew through the base of a 20 m s^{-1} updraft in severe turbulence. The difference between these values is consistent with the innermost saturated thermodynamic measurement’s being an underestimate of the updraft θ_e , although entrainment of low θ_e air into the updraft between 890 and 500 hPa may have lowered θ_e at the higher altitude.

Super Typhoon Flo formed in the monsoon trough, became a typhoon on 15 September 1990, and intensified rapidly to super typhoon the next day (Joint Typhoon Warning Center 1990). Figure 4a shows the eye sounding in Flo at 0500 UTC on 17 September 1991, near the end of the rapid intensification, when Flo’s MSLP was 891 hPa. The sounding extends through a greater depth of the atmosphere, from the surface to 275 hPa. The inversion lies from 720 to 760 hPa. The sounding below the inversion parallels a moist adiabat, but the air is not particularly moist. Its dewpoint depression is 10°C . In the lowest 50 hPa above the surface, the sounding is dry adiabatic. The relatively moist layer may be a “fossil” inversion that was once much like those shown in Figs. 1–3 but was subsequently subjected to an additional 100 hPa of subsidence.

Above the inversion, the dewpoint depression increases to 15°C . This part of the sounding also parallels a moist adiabat up to 425 hPa. Above 425 hPa, θ_e is nearly constant at 370 K. This air appears to have been drawn or mixed into the eye in the upper troposphere. Its thermodynamic properties are consistent with origin in the eyewall followed by descent that reaches only to

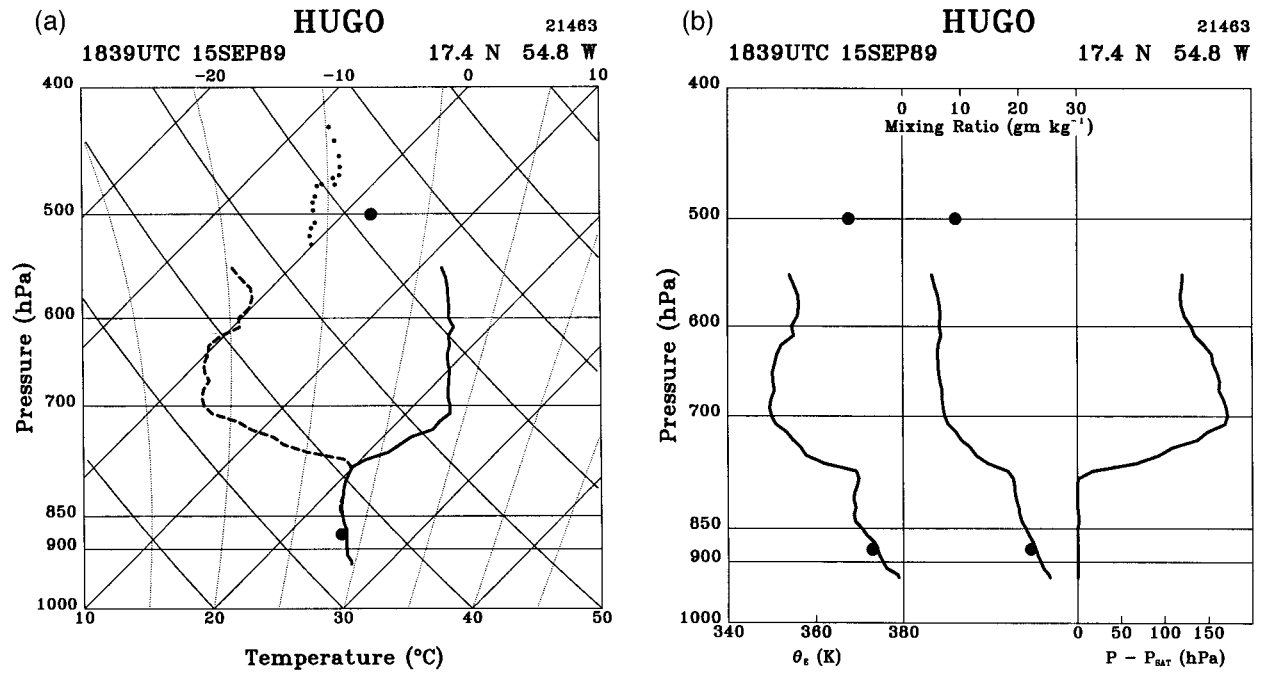


FIG. 3. As in Fig. 1 but for Atlantic Hurricane Hugo at 1839 UTC on 15 September 1989: (a) skew T -log p ; and (b) θ_e mixing ratio, and $P - P_{\text{SAT}}$.

a bit below 400 hPa, not to the surface as in the conventional model. The saturation points define a sounding slightly warmer than the $\theta_e = \sim 350$ K moist adiabat. Above 600 hPa, the difference between T_{SAT} and the 350

K moist adiabat increases from about 1–2 K to more than 10 K. The minimum θ_e in the sounding, 353 K, occurs in two places: at the top of the inversion and also at 840 hPa, the top of the near-surface dry adiabatic

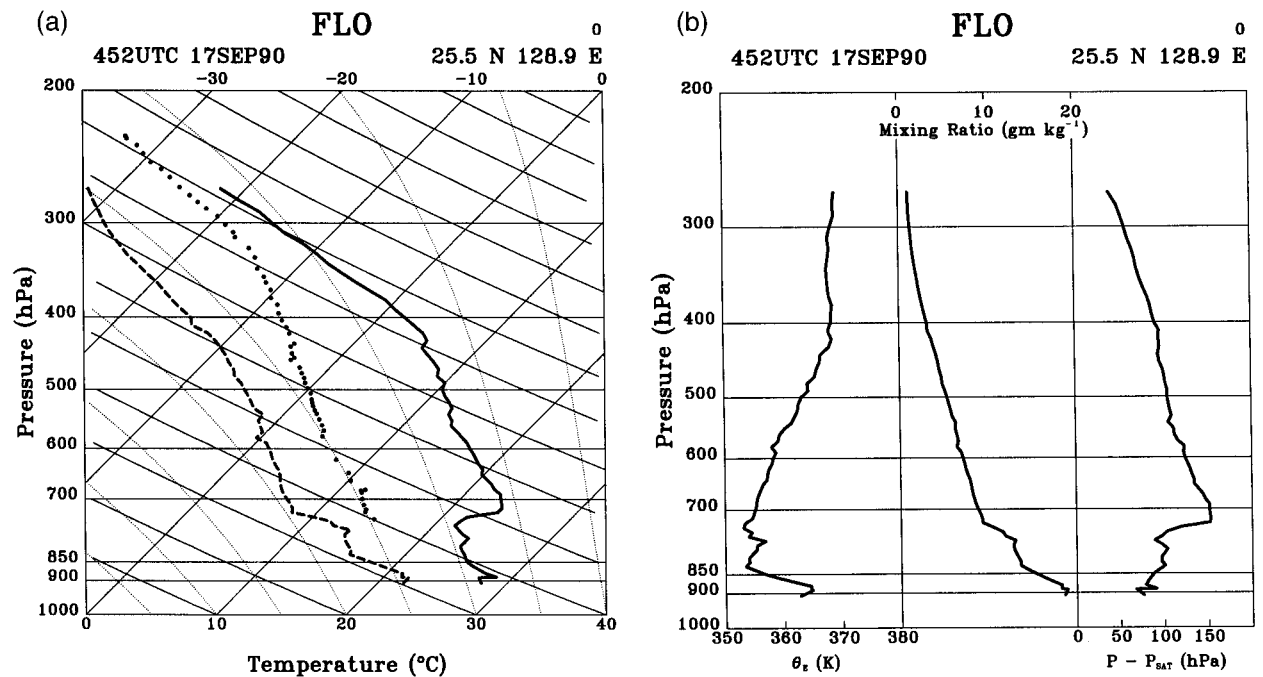


FIG. 4. As in Fig. 1 but for Super Typhoon Flo at 0452 UTC on 17 September 1990: (a) skew T -log p with no eyewall temperature indicated; and (b) θ_e , mixing ratio, and $P - P_{\text{SAT}}$.

TABLE 1. Kinematic calculation of r_{ave} , the vertically averaged separation between the falling drop sondes in Figs. 1–4, and the axis of vortex rotation, based upon $v_{\text{ave}} = \pi r_{\text{ave}} \Delta\lambda / (180^\circ \Delta t)$, where v_{ave} is the average wind speed reported by the sonde in time interval Δt , during which the wind direction changed by amount $\Delta\lambda$.

Storm	Date/time	v_{ave} (m s ⁻¹)	$\Delta\lambda$ (°)	Δt (s)	r_{ave} (m)
Olivia	24/2123	No winds			
	25/2211	8	120	444	1698
Jimena	23/2058	7	90	667	2971
	23/2330	2	420	389	106
Hugo	15/1839	23	255	822	4249
Flo	17/0452	6	110	867	2709

layer. The largest saturation pressure difference, 150 hPa, coincides with the upper θ_e minimum at 720 hPa. Unlike Figs. 1–3, there is no clear evidence of moisture being mixed into Flo's eye in the lower troposphere.

These soundings are unusual only in that they were selected for well-defined inversions somewhat below flight level. Often reconnaissance aircraft operating at 700 hPa fly either at the inversion or in the moist layer, even in intense tropical cyclones. For example, throughout the rapid intensification of Hurricane Opal of 1995, the eye soundings below flight level at 700 hPa were essentially moist adiabatic. Only after Opal attained minimum pressure, 916 hPa, did the inversion descend below flight level. Then, as the storm filled, the inversion rose and thickened. The correlations between lowering of the inversion, warming and drying of the eye, and intensification on one hand and moistening of the eye and filling on the other seem to be common, but not inevitable.

Several considerations affect interpretation of eye-sounding data: representativeness of individual soundings, location of the sounding within the eye, and possible short-term (period ~ 1 h) oscillations of the eye as a whole. Although no examples of multiple simultaneous dropsonde deployments in the eyes of tropical cyclones seem to exist, horizontal profiles of flight-level temperature and dewpoint usually show relatively flat gradients within about half an eye radius of the center and steeper gradients close to the eyewall. It would be worthwhile to drop sondes in pairs to assess repeatability of thermodynamic measurements and also as tracers for the kinematics. Still, if it can be established that the sonde fell near the eye center, the measurements should be representative. Sondes usually spiral downward as they fall through air circulating around the vortex axis. The wind speed and changes of wind direction reported by the sondes can be related kinematically to the distance from the axis of rotation

$$v_{\text{ave}} = \pi r_{\text{ave}} (\Delta\lambda / 180^\circ \Delta t),$$

where r_{ave} is the average distance from the axis and v_{ave} is the average wind speed reported during time interval Δt as the wind direction changed by $\Delta\lambda$ degrees. Table 1 shows results of this calculation that confirm that all sondes with reported winds fell within 5 km of the kin-

ematic center. Given that all of the eyes in question were >10 km in radius, it seems likely that these sondes fell in the region of flat horizontal gradients near the center. Although the sonde in Olivia at 2123 UTC on the 24th failed to report the winds necessary to calculate r_{ave} , the sharp inversion and low humidity in Figs. 1a and 1b are consistent with descent near the axis. Finally, radar observations of Olivia, Jimena, and Hugo showed pulsating convection on a timescale comparable with the orbital period of air moving with the maximum swirling wind. Since this period is not too different from the Brunt–Väisälä period, it would not be surprising if the convection induced axisymmetric, gravity wave oscillations, perhaps with amplitudes as large as tens of meters. Apart from the differences between the two soundings in Jimena, the data show no obvious signatures of this kind of noise, but it is certainly possible that aliased vertical oscillations affect the thermal structure observed in eye soundings.

3. Conceptual model

How does the two-layer thermodynamic structure of the eye come about? Measurements of chemical tracers suggest long residence times for air in the upper reaches of the eye (Newell et al. 1996). Figure 5 illustrates a hypothetical model of the eye in which the air above the inversion has remained in the eye since it was enclosed when the eyewall formed. Under this hypothesis, streamlines emerge from the eyewall near the tropopause, bend downward inside the eye, and rejoin the eyewall in the lower troposphere; but the motion is so slow that the air parcel trajectories do not close. When the eyewall first formed, it enclosed air from the cloud mass of the preexistent tropical storm. The sounding inside might plausibly have been saturated, or nearly so, and dominated by convective adjustment toward a moist adiabat near $\theta_e = \sim 350$ K. Thus, the observed $P - P_{\text{SAT}}$ may represent the total subsidence since the eye formed. In this interpretation, air inside the eye sinks gradually as loss to the eyewall draws mass outward around the bottom of the eye. Dewpoint depressions at the inversion are 10–30 K rather than the ~ 100 K that would occur if the air originated at the tropopause and descended without dilution. The local minimum of θ_e is consistently in the lower troposphere. Its value, >10 K below the observed eyewall θ_e , is difficult to explain if one supposes that the other properties of the air derive from mixing with eyewall air. The hypothesis of 100–200-hPa dry adiabatic forced descent inside the eye eliminates the need for hypothetically large inward mixing of eyewall air to force subsidence and maintain the moisture budget inside the eye (Malkus 1958; Miller 1958).

An average sounding for the environment of Atlantic Hurricanes (Sheets 1969) typically shows minimum θ_e of 339 K at 3–6-km altitude. When the soundings are stratified by surface pressure, the mean of soundings

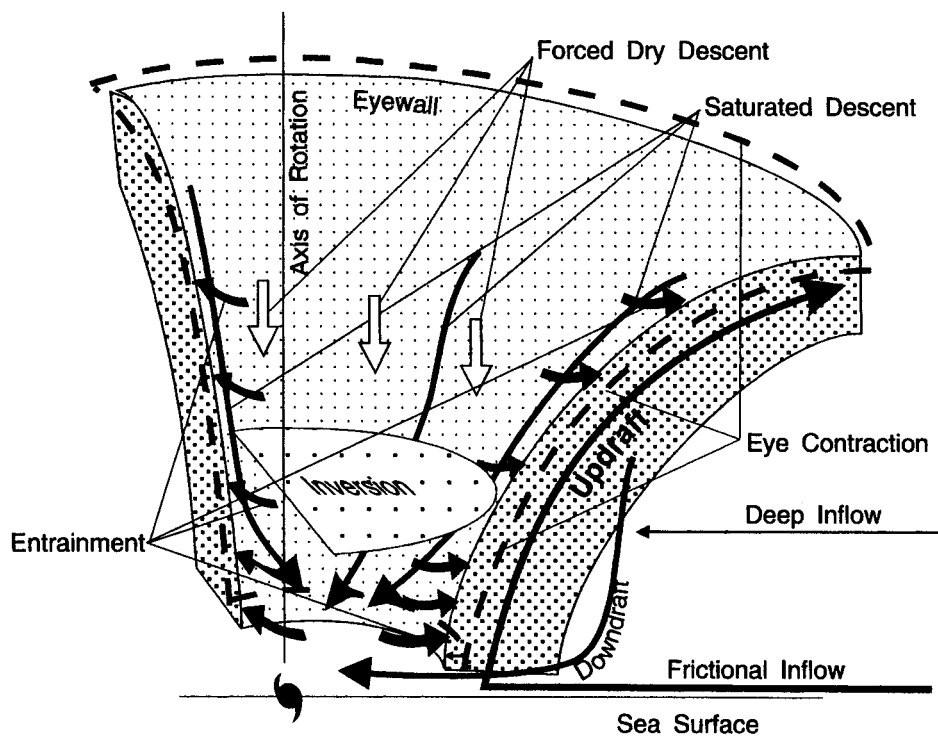


FIG. 5. Schematic illustration of the secondary flow in the eye and eyewall of a hurricane. The frictional indraft feeds the buoyancy-driven primary updraft and outflow in the eyewall cloud. Inflow under the eyewall is derived from convective downdrafts. It, and evaporatively driven descent along the inner edge of the eyewall, feed moist air into the volume below the inversion. Gradual thermodynamically or dynamically driven descent of dry air inside the eye warms the air column adiabatically. The descent is forced as convection draws mass from the bottom of the eye into the eyewall. Balance between moist-air production and loss to the eyewall determines the rate of rise or fall of the inversion.

with surface pressures >1010 hPa shows lower minimum θ_e , 335 K at 3-km altitude; the mean of soundings with surface pressures <995 hPa—which are more strongly influenced by convection—has minimum $\theta_e = 342$ K, also at 3 km. In the latter soundings, θ_e a kilometer or two above the minimum is 345–346 K, still about 5 K cooler than the minimum θ_e observed in the eyes described in section 2. If the Atlantic mean environmental soundings with surface pressures <995 hPa may be taken as representative of the air enclosed during formation of the eyes of these, predominantly Pacific, tropical cyclones, 5–6 km of descent combined with evaporation of about 10 gm kg^{-1} of virga would be required to bring 350 K air from 9 km (where this value of θ_e is found) to the inversion level with the observed temperature and mixing ratio. Alternatively, 40% dilution of 345 K eye air with 365 K eyewall air could produce the same result. Thus, based upon plausible initial soundings, it is possible to argue for more descent and evaporation, or somewhat more mixing from the eyewall into the eye, or both. Nonetheless descent from tropopause height and rapid mixing into the eye appear to be inconsistent with observations.

As shown in Fig. 5, loss of mass to the eyewall might be balanced by shrinking of the eye's volume with little

or no detrainment from the eyewall into the eye in the upper troposphere. The convergence due to shrinking of the eye is $A^{-1}\partial A/\partial t = 2a^{-1}\partial a/\partial t$, where $A = \pi a^2$ is the area for an eye of radius a at some specified altitude and $\partial A/\partial t = 2\pi a\partial a/\partial t$. If during some time interval, the area of the eye were to contract by a half or a third over the depth between 850 and 150 hPa and all of the excess air were to be squeezed downward through the 850-hPa surface, the subsidence at the bottom of the volume would be 500–700 hPa, 3–5 times the subsidence expected from the saturation pressure deficits in Figs. 1–4. The question seems to be not whether eye contraction can supply enough air to explain the subsidence, but rather how to dispose of the excess air supplied by even modest shrinking of the eye.

The subsidence computed from the saturation pressure differences is 100–150 hPa, equivalent to 1–1.5 km of descent. If all of the subsidence happened in two days, the vertical velocity inside the eye would be $\sim 1 \text{ cm s}^{-1}$. If the subsidence happened in 5 days, the velocity would be 0.4 cm s^{-1} . These figures are substantially smaller than the 11 cm s^{-1} subsidence determined by Franklin et al. (1988) in Hurricane Gloria of 1985. But the Gloria observations were unusual because they captured the downward plunge of the inversion as Glo-

ria's MSLP fell 10 hPa in less than 5 h and because the rapid descent was confined to a relatively shallow vertical interval with comparable ascent above the sinking layer. Even though the interval between the soundings was 4 h, much longer than the typical period of variation in eyewall convection, it is still possible that the large apparent subsidence reflected an aliased short-period oscillation superimposed on long-term intensification of the hurricane.

In seeming contradiction with the hypothesis of thermodynamic isolation from the eyewall, some mixing into the eye seems to occur. The shallow layers of moistening and cooling, but increasing θ_e , shown in Figs. 2 and 3, are examples of one kind of mixing that is apparently too weak to dominate the moisture budget. Another mechanism for moistening the eye involves small-scale mixing adjacent to the eyewall. A mixture that contained clear air from the eye and moist air from the eyewall in proportions such that it was just saturated—misty rather than cloudy—would be the coolest and densest possible for specified properties of the original air masses (Betts 1982). Jorgensen's (1984) analysis of in situ aircraft data revealed evaporatively driven descent along the inside edge of the eyewall. Visual observation (e.g., Simpson 1954) and photographs of the eyewall from inside of the eye (Fig. 6a) often show a descending cascade of misty air. Evidently, evaporation of condensate mixed into the eye forms a moist descending boundary layer that appears as a flow of mist or pileus down the inside of the eye into the stratocumulus-topped moist layer. As an aircraft penetrates into the eye, it often experiences a final shudder of turbulence when the eye is visible ahead through a veil of mist after the airplane has emerged from dense cloud. Visual and photographic observations show the clouds on the inward edge of the eye organized into inclined rolls that wind helically around the eye (Bluestein and Marks 1987) that may be a manifestation of shearing instability of the radial wind profile (Emanuel 1984). Thus, the misty layer is turbulent as well as moist. The frequently observed clear "moat" at low level just inside the eyewall (Fig. 6b, Simpson 1952; Simpson and Starrett 1955) may result from the moist descent's flow through the inversion into the moist air below.

Emanuel (1997) builds upon earlier work (Eliassen 1959; Palmén and Newton 1969) to hypothesize that heating in the eyewall causes a collapse toward a thermal and momentum discontinuity at the eye boundary,

analogous to that described in the semigeostrophic theory of frontogenesis. Clearly, mixing into the eye must occur to prevent the collapse—consistent with observations of the misty boundary layer and inclined cloud rolls at the eyewall. If the collapse were not controlled, the swirling velocity would drop discontinuously to zero just inside the radius of maximum wind, so that there would be no cyclostrophic height fall between the wind maximum and the center. Emanuel also offers a mathematical argument that the isobaric height must fall most rapidly in the region of heating at the eye boundary as a "proof" that heating alone cannot raise the temperature at the eye's center above that in the eyewall.

An example of the effect appears in a calculation of Hurricane Allen's intensification [Fig. 16 of Willoughby et al. (1982)] with a frictionless Sawyer-Eliassen equation that reproduces the observed wind increase and geopotential decrease quantitatively [cf. Fig. 15 of Willoughby et al. (1982)] for heating rates consistent with the observed radar reflectivity. The computational results agree in detail with observed changes with two exceptions: In the calculations, the pressure falls 50% more rapidly just inside the eye than it does at the center, and the wind decreases with time around the center of the eye in response to the decreasing pressure gradient. In the observations, the pressure falls most rapidly at the eye center, and the wind increases throughout the eye, though only slowly at the center.

An argument counter to Emanuel's recognizes that the pressure fall at the center is still a substantial fraction of that at the eyewall and that any point at the eyewall will soon be left outside the eye as a result of eyewall contraction. Thus, the instantaneous pressure falls are more rapid at the eye boundary, but they do not last as long. The response to heating alone can force height falls throughout the eye as it makes the wind profile inside the eye increasingly "u-shaped." Mixing is confined to a narrow layer of strong gradients next to the eyewall where it prevents collapse of the gradients to a discontinuity and, incidentally, mixes moisture into the eye to drive the moist cascade at the eyewall. Although mixing is essential to maintenance of a continuous wind profile required for thermally driven descent to occur throughout the eye, it does not necessarily cause the descent.

The moisture below the inversion thus seems to derive in part from condensate mixed across the inside edge of the eyewall, but the other sources may include sea-air interaction inside the eye and frictional inflow under

→

FIG. 6. (a) Photograph inside the eye of Hurricane Olivia at 2136 UTC on 25 September 1993, showing the downward cascade of moist air along the inner edge of the eyewall. The moist boundary layer is most clearly visible along the border between the eyewall and the sky that runs from the left center to the upper right. The eyewall slopes away from the camera so that the line of sight is tangent to it along the border. This geometry renders the cascade more visible because it provides a long optical path in the moist air. The mist visible against the sky derives from cloud and virga mixed a kilometer or two into the eye. (b) Photograph of the hub cloud in Olivia's eye at 2137 UTC. The hub cloud and center of circulation occupy the lower right of the frame with the lower clouds that surround the hub extending from the lower left to the upper right and the clear moat in the upper-left corner (photographs by James Franklin, HRD/AOML).



the eyewall. Jordan (1952) considered these sources, but rejected both—the former on the basis of the supposed lack of outward slope of the eyewall, and the latter because no one believed that vortex translation extended into the eye. It is true that frictional inflow toward the eyewall in the boundary layer decelerates at the wind maximum and most of it turns upward. Nevertheless, the angular momentum budget of the boundary layer implies that as much as 25% of the inflow should pass under the eyewall into the eye. If the eyewall works the same way as outer rainbands (Powell 1990), this inflowing air should be preferentially low θ_e downdraft air so that turbulent transfer from the surface must play an essential role in its reaching the high values of θ_e observed below the inversion. Similarly, if the only source of moist air were converging moist descent along the inner edge of the eye above the surface, it would not be possible for it to converge toward very low angular momentum air at the eye's center without surface friction. As a result of heating from below and surface friction, the air below the inversion in the eye is probably turbulent enough for the moist air from the different sources to be blended quickly. The balance between production of moist air by mixing across the eye boundary, frictional inflow, and local turbulent exchange at the surface, on one hand, and loss of moist air to the eyewall updrafts on the other, determines the depth of the inversion in the eye. If the inversion level rises or descends fairly slowly, the moist air must cycle quickly back into the eyewall to balance the fairly large sources, so that its residence time in the eye is much shorter than that of the dry air above the inversion.

The convective updrafts in the eyewall are buoyant with respect to the air around the eye, but not with respect to the eye itself. Collectively, they act as a “heat pump” that does work on the eye by pulling air out around the bottom of the eye to force thermally indirect descent. Since the updrafts do not rise in the warmest air inside the eye, the warm anomaly that causes the lowest hydrostatic pressure does not necessarily limit eyewall convection. When the convection is intense, net flux from the eye lowers the inversion and promotes descent above the inversion, warming and drying the eye. When the convection weakens, net frictional inflow and mixing into the eye raise the inversion, cooling the eye and filling it with cloud. This interpretation is consistent with the idea that convection causes the pressure fall between the eyewall and the axis of vortex rotation through compensating subsidence and adiabatic warming concentrated in the eye.

4. Synthetic soundings

The foregoing conceptual model provides a framework for generation of synthetic eye soundings based upon temperature and dewpoint at the bottom of the inversion, depth of the inversion, and the amount of subsidence inside the eye, estimated as the maximum

saturation pressure difference at the top of the inversion. The synthesis also requires a “generating sounding,” the sounding in the air that was enclosed, by hypothesis, when the eye first formed and that lies along the locus of the observed saturation points in subsequent eye soundings. This sounding should generally be a bit more stable than the $\theta_e = 350$ K moist adiabat that passes through 25°C (298.16 K) at 1000 hPa. It is generated by computation of a moist adiabat corresponding to a 1000-hPa temperature of 298.16 K + ΔT and then scaling that adiabat by the factor $298.16/(298.16 + \Delta T)$, where ΔT is 3–5 K. Since moist adiabats' lapse rates decrease with increasing θ_e , the scaled adiabat will be more stable than the unmodified moist adiabat passing through 298.16 K. The eye sounding above the inversion derives from the generating sounding by dry adiabatic compression equal to the observed $P - P_{SAT}$ at the inversion level and decreasing linearly (or perhaps quadratically) to zero at the tropopause. Linear decrease is intuitively satisfying because it corresponds to uniform convergence inside the eye. Observed eye soundings below the inversion are moist adiabatic from the base of the inversion to the mixing condensation level and then nearly dry adiabatic to the surface. The synthetic soundings do not retain quite this much detail; they approximate the sounding below the inversion as a moist adiabat that extends from the temperature at the base of the inversion to the surface. It is also possible to specify that the sounding below the base of the inversion has a fixed dewpoint depression as shown in Figs. 1 and 4.

A synthetic sounding corresponding to Fig. 4 appears in Fig. 7. For properly chosen values of the parameters, it is clearly possible to synthesize a given sounding fairly accurately. Nevertheless, one should be careful not to read too much into the result because the synthesis is a quantitative description with a half-dozen disposable parameters rather than a predictive physical model.

The synthetic eye soundings are useful for determination of the hydrostatic pressure fall between the eyewall and the axis of rotation consistent with the hypothetical eye thermodynamics. An upward hydrostatic integration along an assumed saturated adiabatic eyewall sounding yields the 150-hPa height, and a downward hydrostatic integration along the synthetic eye sounding can, if the eyewall surface pressure is chosen appropriately, recover the observed MSLP. The eyewall sounding is the moist adiabat that corresponds to θ_e below the inversion so that the first part of the calculation estimates the (dominant) contribution of convective warming to the total pressure deficit. Iterative adjustment of the eyewall surface pressure, initially assumed to be the observed MSLP plus one-third of the difference between 1013 hPa and the MSLP, changes the 150-hPa height and hence the result of the downward integration. This process converges reliably in a few

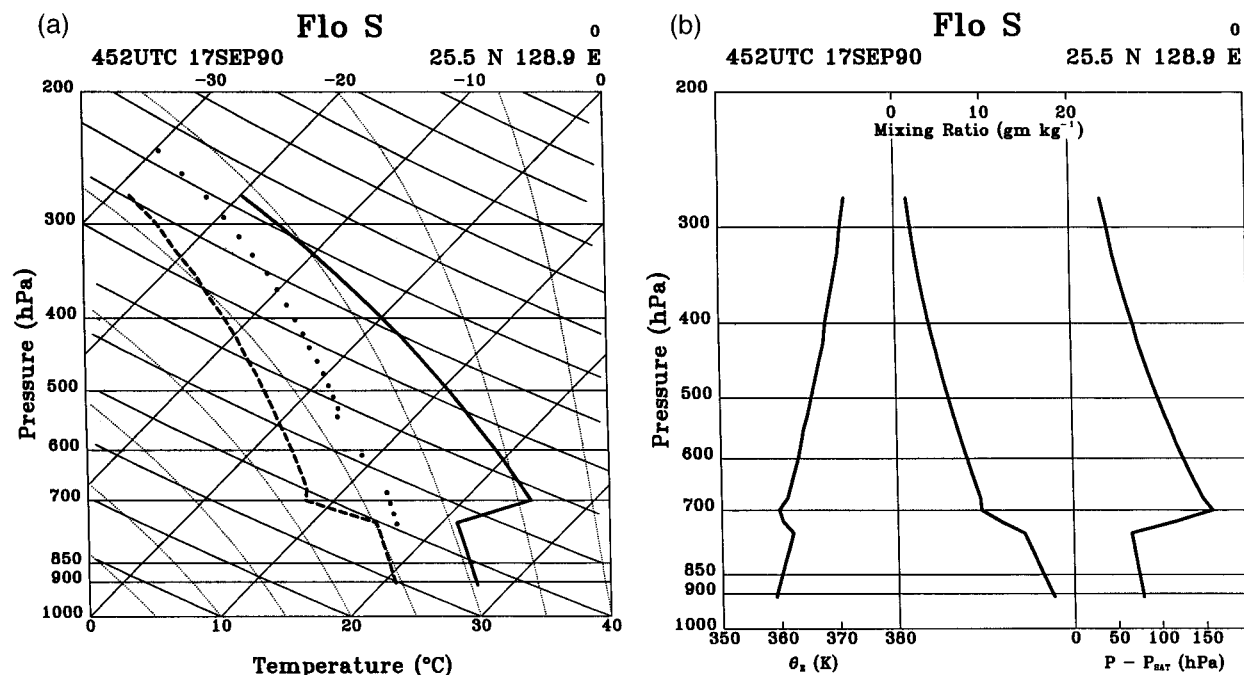


FIG. 7. Synthetic sounding in the eye of Super Typhoon Flo for the time and conditions shown in Fig. 4, illustrated (a) as a skew T -log p diagram; and (b) as graphs of θ_e , mixing ratio, and $P - P_{\text{SAT}}$.

iterations to the observed MSLP because the central pressure is nearly linear in the eyewall surface pressure.

Figure 8 illustrates the pressure decrease from the eyewall to the center of the eye for inversions at 900, 700, and 500 hPa, subsidence at the top of the inversion from 0 to 200 hPa, and linear ($n = 1$) or quadratic ($n = 2$) decrease of subsidence with height above the top of the inversion. The pressure fall increases essentially linearly with descent at the inversion top, and is not particularly sensitive to the level of the inversion. One

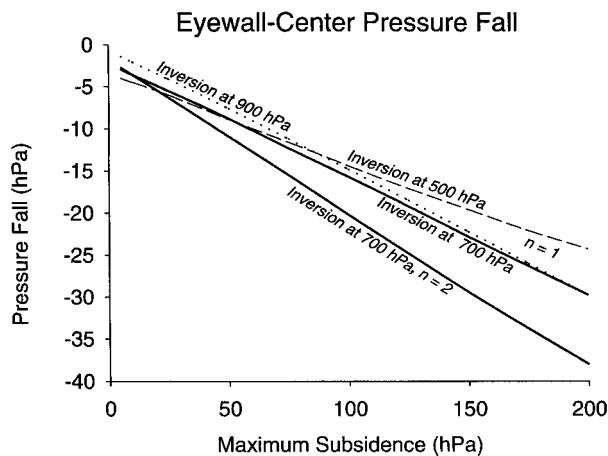


FIG. 8. Pressure fall from the eyewall to the center of the eye as a function of maximum subsidence for inversions at 900 hPa, 700 hPa, and 500 hPa, and for linear ($n = 1$) or quadratic ($n = 2$, 700 hPa only) variation of subsidence with height above the inversion.

would expect that lowering of the inversion in nature would occur with strong subsidence and greater cyclone intensity, as is observed. But as far as the hydrostatic calculation goes, it is primarily the maximum amount of subsidence that determines the pressure fall from the eyewall to the center of the eye. The maximum possible pressure fall for 150 hPa of descent is 20–25 hPa for a linear decrease of subsidence with distance from the inversion and 30 hPa for a quadratic decrease. In the former case, mass convergence is constant with altitude; in the latter case, it increases with altitude above the inversion so that more subsidence and more adiabatic warming occur through a greater depth.

Pressure falls vary nearly linearly with subsidence for a given inversion height. The maximum pressure difference attainable through dry descent is consistent with the observation that a quarter to a third of the total pressure fall in intense tropical cyclones occurs inside the radius of maximum wind. Tropical cyclone intensification thus appears as a two-stage process: Convection, with its roots in the high θ_e boundary layer, transports moist enthalpy extracted from the sea upward to elevate θ_e in the upper troposphere, producing a broad area of low pressure. As the wind increases, dry descent is increasingly localized inside the radius of maximum wind so that the pressure gradient at the edge of the eye tightens and the wind strengthens according to the well-established convective ring model (Willoughby et al. 1982). The dry process does lower the pressure farther, but its most significant effect is to sharpen the pressure

gradients that sustain the strongest winds. This aspect is illustrated clearly when a formerly intense hurricane loses its strong convection over cold water or as a result of an eyewall succession. Well documented examples are Gloria of 1985 (Willoughby 1990) and Gilbert (Black and Willoughby 1992). Aircraft observations showed little temperature anomaly at 700 hPa inside the eyes of these hurricanes after weakening. MSLP rose by 20 and 52 hPa, respectively, as the radial wind profiles lost their sharp peak at the eyewall and became flat. The latter pressure rise is even more than one might expect from reversal of the dry adiabatic warming inside the eye alone.

5. Conclusions

The soundings and interpretation presented here suggest strongly that the thermodynamics of tropical cyclone eyes do not obey conventional models in which air detrains from the eyewall near the tropopause, sinks through most of the depth of the troposphere inside the eye—acquiring moisture and momentum as needed to maintain its bulk properties—and is entrained back into the eyewall at the bottom. Conventional models assume implicitly that the time required to cycle air through the eye is short compared with the lifetime of the eye.

The present observations show that the eye contains two air masses separated by an inversion. The air below the inversion exchanges momentum and moist enthalpy with the sea and mixes in complicated ways with air from the eyewall. The air above the inversion has been in the eye since the eye first formed. Its thermodynamic structure may be derived from an initial sounding a bit more stable than a moist adiabat to which is applied a total subsidence of a kilometer or two—or at most a few kilometers if evaporational or radiational cooling is significant. The saturation pressure difference is a conservative estimate of the total descent. Radiation or evaporation of virga falling into the eye may moisten the air and might conceivably cool the sounding by $>10^{\circ}\text{C}$, equivalent to more than a kilometer of additional subsidence. Inward mixing of eyewall air may also increase θ_e by a few degrees above the midtropospheric values in the original eye sounding. Still these effects cannot hide enough subsidence to bring air from the tropopause at 15–16 km to the inversion top at 1–3 km. It is difficult to explain the θ_e minimum, $>10\text{ K}$ below the eyewall θ_e , if one believes in rapid inward mixing from the eyewall over short timescales compared with the 2–5 days required for significant radiative cooling.

The subsidence in the eye comes about as the eye of the intensifying tropical cyclone contracts—as it is observed to do and as described by balanced models. Incorporation of eye air into both the moist downward cascade inside the eye and the convective updrafts in the eyewall above the inversion accounts for the mass lost as the eye contracts. The net loss is larger

near the bottom of the eye. It thus forces about a centimeter per second of subsidence and gradual adiabatic warming and drying of the eye. Warming through this mechanism can account for no more than 30 hPa of pressure fall from the radius of maximum wind to the eye's center.

Acknowledgments. Discussions with P. Black, K. Emanuel, and G. Holland informed my ideas on this topic, though they may well disagree with some of my interpretation. I also thank B. Albrecht, K. Emanuel, D. Churchill, J. Franklin, J. Gamache, and G. Holland for thoughtful comments that greatly improved the manuscript. It is with sorrow that I note the recent passing of C. L. Jordan whose pioneering work has shaped my thought on eye thermodynamics since I first read it as a student. This research was supported under ONR Grant N00014-94-F-0045.

REFERENCES

- Betts, A. K., 1982: Saturation point analysis of moist convective overturning. *J. Atmos. Sci.*, **39**, 1484–1505.
- , and M. F. Silva Dias, 1979: Unsaturated downdraft thermodynamics in cumulonimbus. *J. Atmos. Sci.*, **36**, 1061–1071.
- Black, M. B., and H. E. Willoughby, 1992: Concentric eyewall cycle of Hurricane Gilbert. *Mon. Wea. Rev.*, **120**, 947–957.
- Bluestein, H. B., and F. D. Marks, 1987: On the structure of the eyewall of Hurricane Diana (1984): Comparison of radar and visual observations. *Mon. Wea. Rev.*, **115**, 2542–2552.
- Case, B., and M. Mayfield, 1990: Atlantic hurricane season of 1989. *Mon. Wea. Rev.*, **118**, 1165–1177.
- Eliassen, A., 1959: On the formation of fronts in the atmosphere. *The Atmosphere and Sea in Motion*, B. Bolin, Ed., Oxford University Press, 227–287.
- Emanuel, K. A., 1984: A note on the stability of columnar vortices. *J. Fluid Mech.*, **145**, 235–238.
- , 1986: An air–sea interaction theory for tropical cyclones. Part I: Steady-state maintenance. *J. Atmos. Sci.*, **43**, 585–604.
- , 1997: Some aspects of hurricane inner-core dynamics and energetics. *J. Atmos. Sci.*, **54**, 1014–1026.
- Franklin, J. L., S. J. Lord, and F. D. Marks Jr., 1988: Dropwindsonde and radar observations of the eye of Hurricane Gloria (1985). *Mon. Wea. Rev.*, **116**, 1237–1244.
- Holland, G. J., 1997: The maximum potential intensity of tropical cyclones. *J. Atmos. Sci.*, **54**, 2519–2541.
- Joint Typhoon Warning Center, 1990: Annual tropical cyclone report. JTWC, 144–151. [NTIS AD A 239910.]
- Jordan, C. L., 1952: On the low-level structure of the typhoon eye. *J. Meteor.*, **9**, 285–290.
- , 1961: Marked changes in the characteristics of the eye of intense typhoons between the deepening and filling stages. *J. Meteor.*, **18**, 779–789.
- Jorgensen, D. P., 1984: Mesoscale and convective-scale characteristics of mature hurricanes. Part II: Inner core structure of Hurricane Allen (1980). *J. Atmos. Sci.*, **41**, 1287–1311.
- Kessler, E., II, 1958: The eye region of Hurricane Edna, 1954. *J. Meteor.*, **15**, 264–270.
- Malkus, J. S., 1958: On the structure and maintenance of the mature hurricane eye. *J. Meteor.*, **15**, 337–349.
- Miller, B. I., 1958: On the maximum intensity of hurricanes. *J. Meteor.*, **15**, 184–195.
- Newell, R. E., and Coauthors, 1996: Atmospheric sampling of super typhoon Mireille with NASA DC-8 aircraft on September 27, 1991, during PEM-West A. *J. Geophys. Res.*, **101** (D1), 1853–1871.

- Ooyama, K. V., 1969: Numerical simulation of the life cycle of tropical cyclones. *J. Atmos. Sci.*, **26**, 3–40.
- , 1982: Conceptual evolution of the theory and modeling of the tropical cyclone. *J. Meteor. Soc. Japan*, **60**, 369–380.
- Palmén, E., and C. W. Newton, 1969: *Atmospheric Circulation Systems*. Academic Press, 603 pp.
- Pasch, R. J., and M. Mayfield, 1996: Eastern North Pacific hurricane season of 1994. *Mon. Wea. Rev.*, **124**, 1579–1590.
- Powell, M. D., 1990: Boundary layer structure and dynamics of outer hurricane rainbands. Part II: Downdraft modification and mixed layer recovery. *Mon. Wea. Rev.*, **118**, 918–938.
- Rappaport, E. N., and M. Mayfield, 1992: Eastern North Pacific hurricane season of 1991. *Mon. Wea. Rev.*, **120**, 2697–2708.
- Schubert, W. H., and J. J. Hack, 1982: Inertial stability and tropical cyclone development. *J. Atmos. Sci.*, **39**, 1687–1697.
- Shapiro, L. J., and H. E. Willoughby, 1982: The response of balanced hurricanes to local sources of heat and momentum. *J. Atmos. Sci.*, **39**, 378–394.
- Sheets, R. C., 1969: Some mean hurricane soundings. *J. Appl. Meteor.*, **8**, 134–145.
- Simpson, R. H., 1952: Exploring the eye of Typhoon “Marge,” 1951. *Bull. Amer. Meteor. Soc.*, **33**, 286–298.
- , 1954: Structure of an immature hurricane. *Bull. Amer. Meteor. Soc.*, **35**, 335–350.
- , and L. G. Starrett, 1955: Further studies of hurricane structure by aircraft reconnaissance. *Bull. Amer. Meteor. Soc.*, **36**, 459–468.
- Willoughby, H. E., 1990: Temporal changes in the primary circulation in tropical cyclones. *J. Atmos. Sci.*, **47**, 242–264.
- , and M. B. Chelmos, 1982: Objective determination of hurricane tracks from aircraft observations. *Mon. Wea. Rev.*, **110**, 1298–1305.
- , J. A. Clos, and M. G. Shoreibah, 1982: Concentric eye walls, secondary wind maxima, and the evolution of the hurricane vortex. *J. Atmos. Sci.*, **39**, 395–411.